

# Influence of Crack Depth on Performance of Geosynthetic-Reinforced Asphalt Overlays



V. Vinay Kumar and Sireesh Saride

**Abstract** The influence of crack depth in the existing pavement layer on the performance of geosynthetic-reinforced asphalt overlays against reflective cracking is evaluated in this study. The two-layered asphalt beam specimens having a crack depth of 40, and 25 mm in the bottom layer are tested under repeated load four-point bending test to understand the influence of crack depth on the performance of geosynthetic-reinforced asphalt overlays. A digital image analysis technique was incorporated to study the failure modes of unreinforced and geosynthetic-reinforced specimen. Two different types of geosynthetic interlayers, namely woven geo-jute mat (GJ) and a biaxial polypropylene grid with a square aperture size of 40 mm (PP), are used in the study. The repeated loading tests were conducted on all the specimens under four-point bending configuration in a load-controlled mode at a frequency of 1 Hz. The performances of reinforced specimens were compared with the unreinforced specimen (CS), and the improvement in fatigue life was estimated. Fatigue test and DIC results indicate that the reinforced specimens improved the fatigue life of overlays, irrespective of crack depth and among them, the performance of PP specimens is superior. A superior performance of geosynthetic interlayers is witnessed at a larger crack depth (40 mm), irrespective of the interlayer type.

**Keywords** Geosynthetic interlayers · Crack depth · Asphalt overlays · Digital image correlation

---

V. Vinay Kumar · S. Saride (✉)  
Department of Civil Engineering, Indian Institute of Technology Hyderabad,  
Kandi, Sangareddy 502285, Telangana, India  
e-mail: [sireesh@iith.ac.in](mailto:sireesh@iith.ac.in)

V. Vinay Kumar  
e-mail: [christite.vinay@gmail.com](mailto:christite.vinay@gmail.com)

© Springer Nature Singapore Pte Ltd. 2019  
R. Sundaram et al. (eds.), *Geotechnics for Transportation Infrastructure*,  
Lecture Notes in Civil Engineering 29,  
[https://doi.org/10.1007/978-981-13-6713-7\\_15](https://doi.org/10.1007/978-981-13-6713-7_15)

## 1 Introduction and Background

The flexible pavements over a period of their service life develop various types of distress due to innumerable detrimental factors such as varying weather conditions, high traffic wheel loads and weak subgrade, and other pavement layer conditions. These distresses result in the reduction in the pavement serviceability and necessitate an immediate need for a rehabilitation program to restore the pavement serviceability. The most common and convenient technique employed to restore the serviceability of deteriorated pavements is by providing an hot mix asphalt overlay of sufficient thickness (Kumar et al. 2017; Kumar and Saride 2017). The HMA overlays are believed to improve the ride quality by reducing the roughness of pavement surface. However, the incorporation of HMA overlays on an existing distressed pavement surface is witnessed to be an interim solution, as the distress from the existing pavement reflects onto the new overlays within a transient duration. This phenomenon of reflection of cracks and distress into and through the new overlays is known as reflective cracking (Kumar and Saride 2018). The major factors influencing the rate of reflective cracking in asphalt overlays are temperature variations and repeated traffic loads (Cleveland et al. 2002). Further, the reflection cracks are often observed to result in the premature failure of the pavement system, as they allow moisture ingress into the layers below through the cracks (Elseifi and Al-Qadi 2003).

Reflective cracking phenomenon is regarded as a complex phenomenon, due to the innumerable influencing factors and hence cannot be completely arrested. Besides, there are a number of possible treatment techniques to retard the rate of cracking in asphalt overlays. Among the various treatment techniques available to restrict the crack growth into the overlays, the inclusion of a geosynthetic interlayer below the asphalt overlay is found to be effective, due to their stress absorbing and reinforcing effects (Elseifi 2003; Saride and Kumar 2017).

There are numerous test methods such as TTI overlay test (Cleveland et al. 2002), Wheel reflective cracking device (Prieto et al. 2007), UGR-FACT (Moreno-Navarro and Rubio-Gamez 2014) available to evaluate the effectiveness of various geosynthetic interlayers as an anti-reflective cracking system. Besides, researchers (Caltabiano 1990; Brown et al. 2001; Virgili et al. 2009; Ferrotti et al. 2012; Kumar and Saride 2017; Saride and Kumar 2017) have studied the effectiveness of various geosynthetic interlayers as an anti-reflective cracking system under flexural fatigue tests.

Based on the existing literature, it can be summarized that the geosynthetics are placed between the new asphalt layers. However, in general, the interlayers will be placed at the interface of old and new pavement layers, to restrict the reflection cracking. Hence, in the current study, the unreinforced and geosynthetic-reinforced asphalt overlays are placed on an old deteriorated pavement extruded during a highway rehabilitation project. The main objective of the study was to evaluate the influence of crack depth on the performance of geosynthetic-reinforced asphalt overlays using repeated four-point bending tests and digital image analysis.

## 2 Materials and Methods

### 2.1 Geosynthetic Interlayers

Two different types of geosynthetic interlayers, namely woven geo-jute mat (GJ) and biaxial polypropylene grid (PP), have been considered in the current study to understand the influence of crack depth on the performance of geosynthetic-reinforced asphalt overlays. To understand the working mechanical and tensile properties of the geosynthetic interlayers, wide width tensile strength tests were performed on both machine (MD) and cross-machine (CMD) directions as per ASTM D4595 (2009). The tensile strength characteristics of the interlayers are discussed in detail in the subsequent paragraphs to follow.

Woven geo-jute (GJ) mat comprises of natural jute fibers and threads. Figure 1 presents the geo-jute mat prepared by machine weaving. The GJ interlayer has an ultimate tensile strength of 25 kN/m (MD) at a strain of 5% and 20 kN/m (CMD) at a strain of 13%. The biaxial polypropylene grid (PP) is manufactured by extending the polypropylene material along the machine and cross-machine directions (MD and CMD) to obtain a square aperture of 40 mm. The biaxial grid has a rib thickness of 2 mm along both the MD and CMD as shown in Fig. 2. The PP interlayer has an ultimate tensile strength of 30 kN/m at a strain of 10–12%.

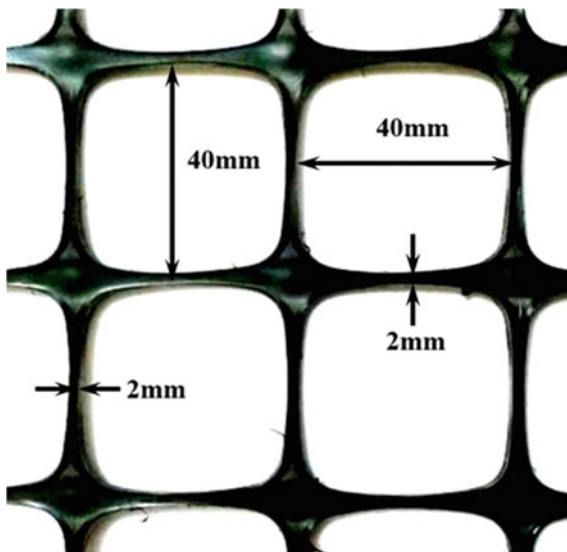
### 2.2 Binder Tack Coat and Asphalt Concrete

The binder tack coat adopted in the study is a penetration grade (PG) 60/70 bitumen. The binder has a penetration value of 66 and a specific gravity of 1.01. The binder has a softening point, flash point, and fire points of 52, 340, and 360 °C,

**Fig. 1** Woven geo-jute (GJ) mat interlayer



**Fig. 2** Biaxial polypropylene grid (PP)

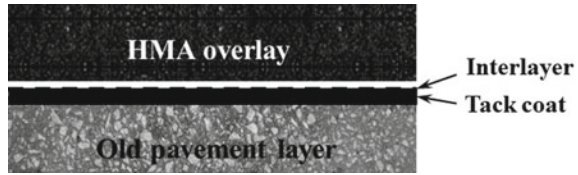


respectively. In addition, a binder viscosity of 400 cP has been reported. The adopted asphalt concrete mix consists of a PG-60/70 binder and a maximum aggregate of 25 mm size. Marshall Stability tests were performed on the asphalt concrete mix, and the optimum binder content of the mix was found to be 5.5% by weight of the aggregates. The asphalt concrete mix with an optimum bitumen content has a strength and flow values of 14.25 kN and 2.5 mm, respectively.

### ***2.3 Two-Layered Asphalt Specimen Preparation***

The two-layered asphalt slab of 400 mm length, 300 mm width, and 90 mm thickness consists of a 45-mm-thick old pavement layer, a binder tack coat, a geosynthetic interlayer and a 45-mm-thick HMA overlay. The old distressed pavement block was extruded from an existing highway during rehabilitation project and cut into a dimension of 400 mm length, 300 mm width, and 45 mm thickness. A PG-60/70 binder tack coat is applied on the old pavement layer at a residual rate of 0.25 kg/cm<sup>2</sup> and then the geosynthetic interlayers as per experimental program. Further, the asphalt concrete mix is compacted with the help of a 5-kg static weight compactor having a height of fall of 500 mm. The two-layered asphalt slabs (Fig. 3) with and without geosynthetic interlayers were then cut into the beam specimens of 400 mm length, 50 mm width, and 90 mm thickness. To understand the influence of crack depth on the performance of geosynthetic-reinforced asphalt overlays, a notch was created in the old pavement layer. The notch depths were of two sizes, i.e., 40 and 25 mm. These depths correspond to about 90 and 55% of the bottom layer thickness, respectively.

**Fig. 3** Schematic of two-layered asphalt slab



Further, the specimens were prepared for the digital image analysis by completely painting one of the specimen faces with white color and spraying a black paint under controlled pressure to create a uniform random speckle pattern. The random speckle pattern on the specimens helps to understand the displacement and strain fields in the specimens. The detailed specimen preparation procedure is explained by Saride and Kumar (2017), Kumar and Saride (2017), and Kumar and Saride (2018).

### 3 Experimental Program

#### 3.1 Flexural Fatigue Test

The flexural fatigue tests were performed on the asphalt beam specimens with different notch depths, under load-controlled mode. Figure 4 presents the schematic of flexural fatigue test setup, and the load was applied with the help of a computer-controlled servo-hydraulic actuator system. A continuous haversine-type loading pattern was applied at a frequency of 1 Hz with an intention to create a live moving traffic (single-axle contact pressure of 550 kPa). In this regard, the maximum load to be applied was calculated using Eq. 1 (ASTM D7460 2010) and it was determined to be 0.6 kN.

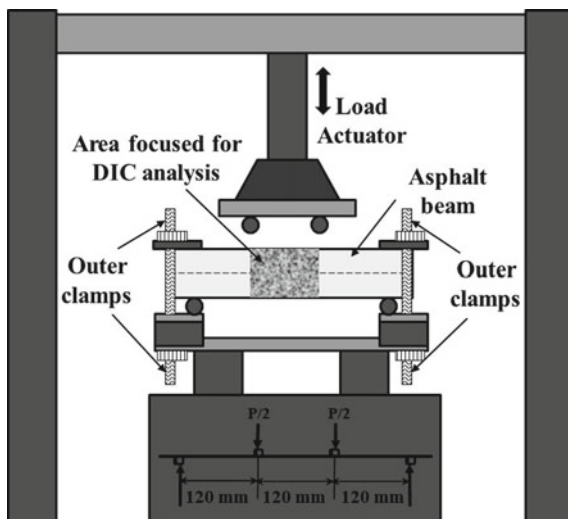
$$\sigma_f = \frac{Pl}{bh^2} \quad (1)$$

where  $\sigma_f$  is the maximum flexural stress in kPa,  $P$  is the maximum load applied in kN,  $l$  is the span length of beam in m,  $b$  and  $h$  are the width and thickness of the beam in m.

A maximum load of 0.6 kN and a seating load of 0.06 kN was applied continuously on the notched beam specimens until complete fracture, and the corresponding vertical deformations at the mid-span length were recorded at the end of every load cycle. These vertical deformations could be adopted in the maximum strain equation to estimate the maximum tensile strains based on the bending theory as per ASTM D7460 (2010).

Further, to understand the crack growth characteristics in the two-layered asphalt beam specimens, a two-dimensional, non-contact optical technique has been employed.

**Fig. 4** Schematic of flexural fatigue test setup



### 3.2 Digital Image Correlation (DIC) Technique

Digital image correlation is a non-contact, optical technique based on the image processing and numerical computing generally employed to measure the full-field displacements effectively. Further, based on the displacement field, the corresponding strains mobilized in the specimen can be determined. The basic principle of the DIC technique is to identify the changes in speckle pattern of the deformed images with respect to that of an undeformed reference image. The process of image recording consists of recording an undeformed reference image and a calibration image before applying the repeated loads. The calibration image is recorded in order to convert the image scale from pixel units to millimeters unit. The images are recorded continuously during the testing at different number of load cycles and are analyzed with the help of commercial software tool (VIC-2D) to study the crack growth characteristics along with the corresponding deformations and strains mobilized in the two-layered asphalt beam specimens.

## 4 Results and Discussion

### 4.1 Flexural Fatigue Test Results

The load-controlled notched beam fatigue tests help to understand the impact of different crack depths on the performance of geosynthetic-reinforced asphalt overlays placed on an old distressed pavement layer. The repeated load was applied continuously on the two-layered notched asphalt beam specimen resulting in an

increase in the vertical deformation of the specimen, with an increase in the number of load repetitions. The increase in vertical deformation causes the dissipation of energy from the specimen and reduces the specimen stiffness, which further results in complete fracture (failure) of the specimen (Kumar and Saride 2017).

The flexural fatigue test results of two-layered asphalt beam specimens with 40 and 25 mm notch depths are presented in Fig. 5, in the form of variation of vertical deformation, as a function of number of load cycles ( $N$ ). It is observed that, the control specimen (CS) could not successfully resist a large number of load repetitions in both the configurations, i.e., cracks propagated into the overlays at a very less number of load cycles ( $N$ ). However, as expected, the specimens with 25-mm notch depth were capable of resisting a large number of load cycles, in comparison with the specimens with 40 mm notch depth. For instance, the fatigue life ( $N$ ) of specimens with 25 mm notch depth is 66, 115, and 674 for CS, GJ, and PP specimens, respectively.

However, the specimens with 40-mm notch depth possess a fatigue life of 14, 33, and 323, for control, GJ, and PP specimens, respectively. The variation in fatigue life of beam specimens with different notch depths may be attributed to their flexural stiffness, which is higher for 25 mm notched specimens followed by 40 mm notched specimens.

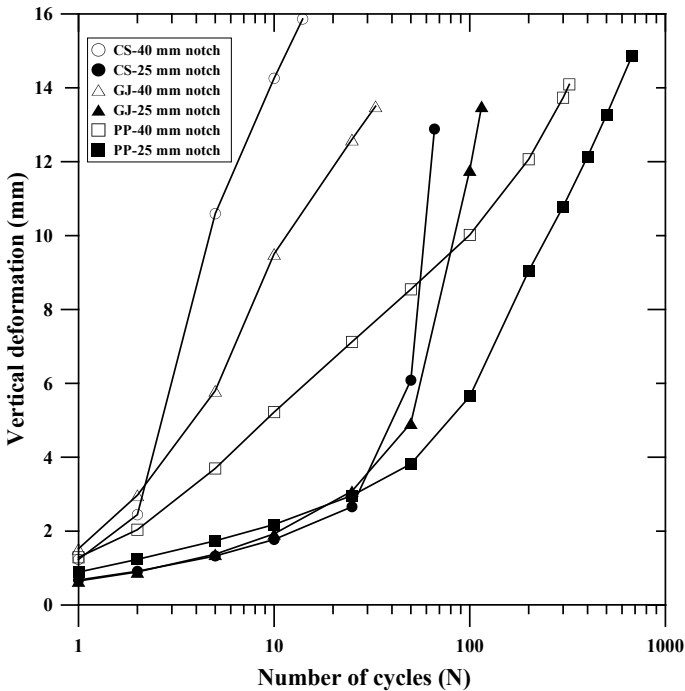


Fig. 5 Variation of vertical deformation with number of cycles

From Fig. 5, it can also be visualized that the specimens with geosynthetic interlayers have shown higher fatigue life, irrespective of the notch depths in the bottom layer. This finding suggests that the geosynthetic reinforcements incorporated in the notched asphalt beam specimens have restricted the vertical deformations and cracks, in turn, enhancing the performance life. Among the specimens with geosynthetic interlayers, the fatigue life of PP specimens is superior to that of GJ specimens, irrespective of the notch depth. Besides, the fatigue life of GJ specimen is observed to be slightly better than that of control specimens. The superior performance of PP specimens may be attributed to their high initial stiffness and their ability to induce an ultimate tensile strength of 36 kN/m at a strain of 10%.

Overall, the geosynthetic interlayers incorporated at the interface of old and new asphalt layers intervene with the crack growth in the vertical direction, by absorbing the crack energy (tensile). In addition, the crack growth is dissipated in the lateral direction at the interface zone by the geosynthetic interlayers. Hence, an improvement in the fatigue life is witnessed.

Further, to quantify the rate of improvement in the geosynthetic-reinforced asphalt beam specimens, a performance indicator is introduced. The performance indicator, improvement ratio is denoted by the term  $I_{NF}$  and is defined as a ratio of number of load repetitions sustained by a geosynthetic-reinforced beam specimen to that sustained by a control specimen, at same vertical deformation level, and mathematically expressed as presented in Eq. 2.

$$I_{NF} = \frac{N_R}{N_U} \quad (2)$$

where  $N_R$  and  $N_U$  are the fatigue lives of geosynthetic-reinforced and unreinforced specimens, respectively.

Figure 6 presents the variation of fatigue life improvement ratio with vertical deformation for all the notched asphalt beam specimens. It can be visualized that the  $I_{NF}$  has increased with an increase in the vertical deformation, irrespective of the notch depth and the geosynthetic-interlayer type. Besides, a prominent performance improvement can be witnessed in asphalt specimens with 40 mm notch depth against the specimens with 25 mm notch depth. This finding can be attributed to the stiffness of the asphalt beam specimens, as the control specimen with a 25-mm notch depth has resisted a large number of load cycles in comparison with the control specimen with a 40-mm notch depth. Hence, a reduction in the improvement ratio can be witnessed. In this regard, it is also clear that, the PP specimen with a 40-mm crack depth had achieved an improvement ratio of about 5.4 against an improvement ratio of 2.2 in PP specimen with a 25-mm notch depth, at 6-mm vertical deformation. Further, an important observation to be noted is that, the improvement ratios of PP specimen with a 40-mm notch depth have been increased after a vertical deformation of 4 mm is reached. It is believed that, at about 4-mm deformation, the crack would have reached the interlayer, and hence, a smooth transfer of strain energy from the cracks takes place and the specimen can resist a higher number of load repetitions.



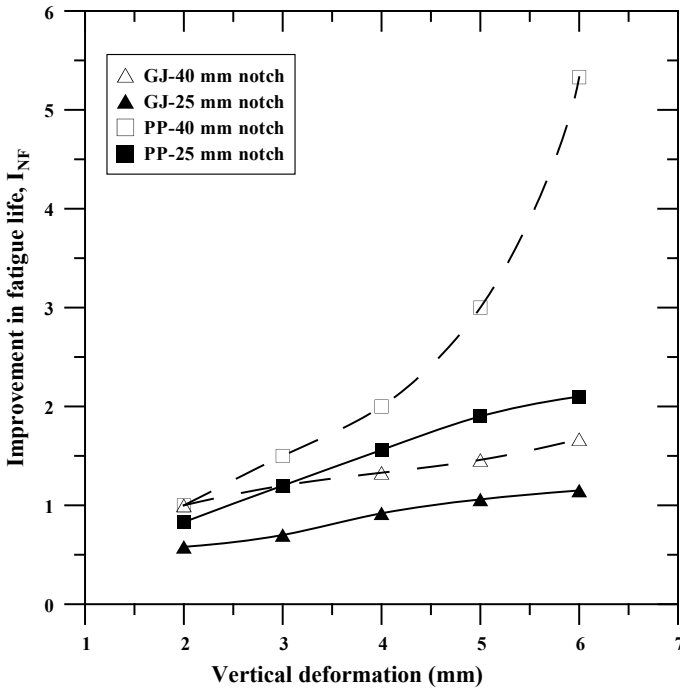


Fig. 6 Variation of fatigue life improvement ratio with vertical deformation

However, a detailed information about the crack growth characteristics in unreinforced and geosynthetic-reinforced asphalt beam specimens with 40 and 25 mm notch depths can be obtained by using the DIC technique, as presented in the following section.

### 4.2 DIC Analysis

The digital image correlation technique was adopted during the flexural fatigue test program with an intention to understand the crack evolution and the propagation patterns. The deformed images after different load cycles are compared with that of undeformed image and the variation in deformation is obtained in the form of vertical deformation bands. Figure 7 presents the variation of vertical deformation bands for all the specimens at failure. The downward deformation is considered to be negative for the analysis, and it can be visualized that each vertical bands represent a uniform deformation in that vertical strip along the specimen. Further, it is to be noted that in the control specimens, the deformation bands are continuous, whereas they are found discontinuous in the specimens with geosynthetic interlayers. This condition may be attributed to the incorporation of geosynthetics at the interface of old and new

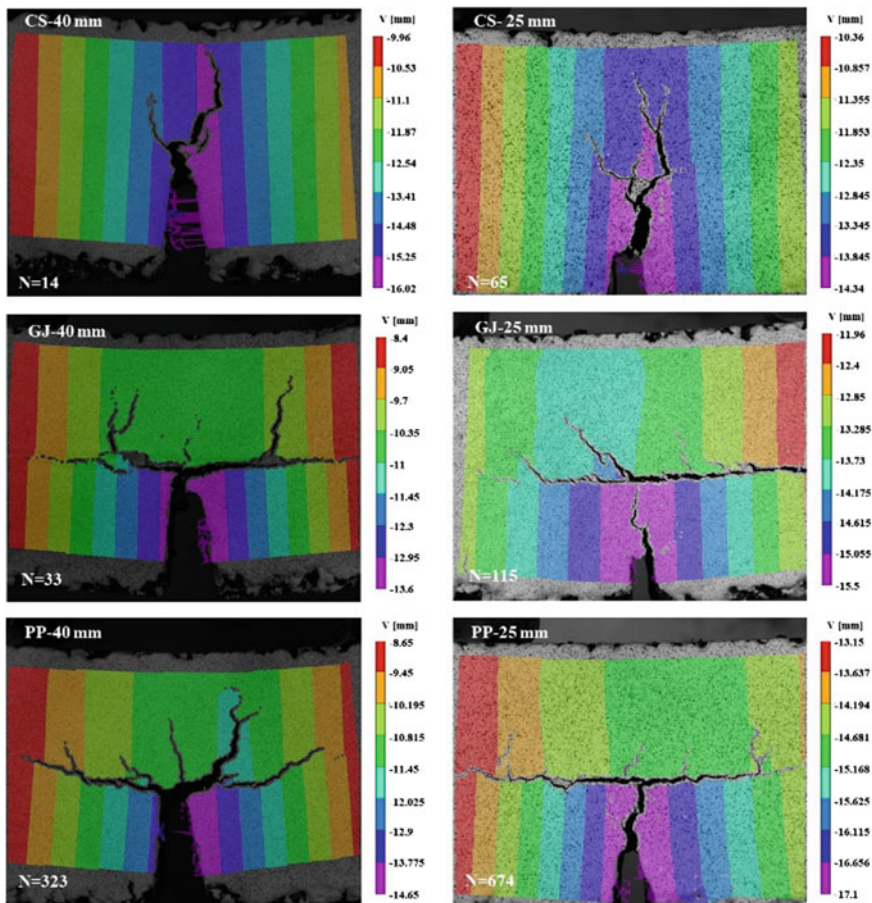


Fig. 7 Variation of vertical deformation bands for all the specimens at failure

pavement layers. The geosynthetic interlayers restrict the vertical deformation and in turn the crack propagations effectively. Hence, maximum vertical deformations are observed in the bottom layer, below the interlayer zone.

The geosynthetic interlayer incorporated below the asphalt overlay effectively restricts the vertical crack growth by minimizing the maximum tensile strains mobilized in the specimen. Figure 8 presents the tensile strain contours at failure condition for all the specimen configurations. It is clear that the tensile strain for the control specimen is consistently higher, irrespective of crack depth. A tensile strain as high as 74 and 33% in control specimens with 40 and 25 mm notch depths, respectively. Besides, low tensile strains are witnessed in the geosynthetic-reinforced notched asphalt beam specimens, irrespective of crack depth. In addition, a maximum tensile strain is witnessed consistently, in the asphalt beam specimens with 40-mm notch depth, irrespective of the geosynthetic-interlayer type.

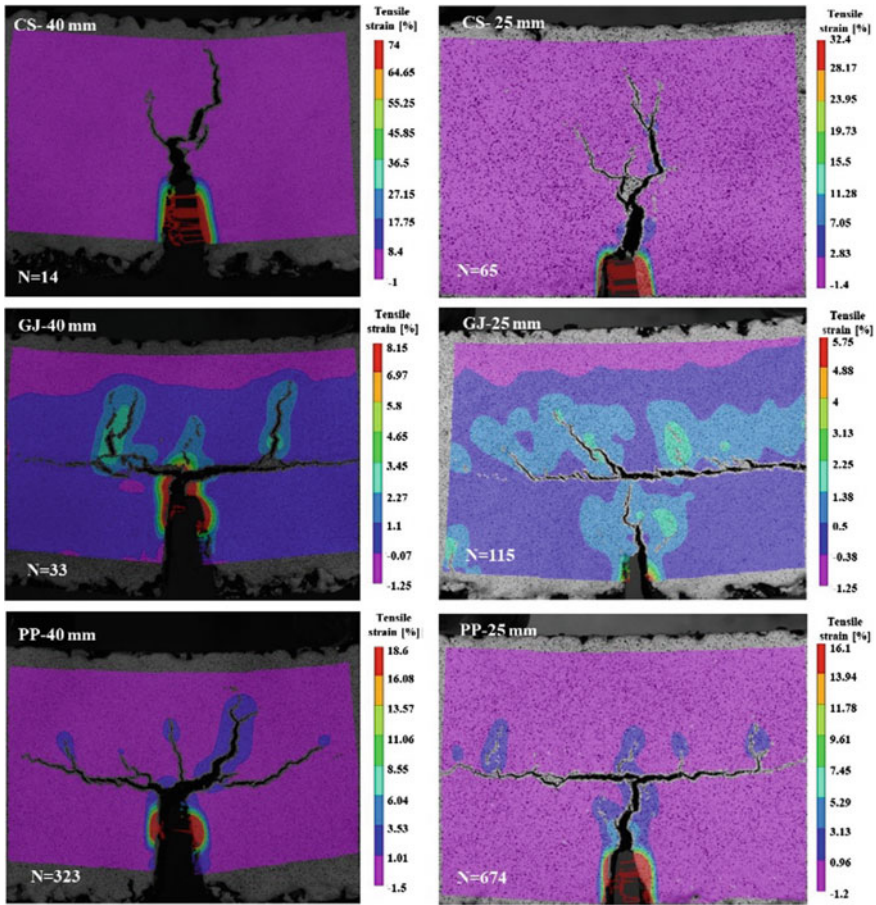


Fig. 8 Variation of tensile strain contours for all the specimens at failure

Further, the maximum tensile stress responsible for vertical crack growth is effectively absorbed by the geosynthetic reinforcements incorporated at the interface zone. Besides, this mechanism of geosynthetic reinforcements often results in a horizontal crack growth below the geosynthetics interlayer, at the interface zone. This condition can be clearly witnessed from Figs. 7 and 8. The crack growth in horizontal direction leads to the accumulation of vertical strains at the interface zone resulting in a possible delamination of pavement layers at the interface zone.

Overall, it can be incurred that there is an enhancement in the performance life of asphalt overlays with the incorporation of geosynthetic reinforcements. Among the notched beam specimens, a maximum improvement is witnessed in asphalt beam specimens with 40-mm notch depth, irrespective of geosynthetics type. Besides, among the geosynthetic-reinforced asphalt beam specimens, a superior performance was witnessed in PP specimens, irrespective of notch depth.

## 5 Conclusions

The influence of crack depth on the performance of geosynthetic-reinforced asphalt overlays placed on a pre-cracked pavement layer was studied under flexural fatigue tests with the help of digital image analyses, and the following conclusions can be drawn:

- All the geosynthetic interlayers improved the fatigue lives of two-layered asphalt beam specimens, irrespective of notch depth in the bottom layer. Among them, the performance of PP specimens is superior to the GJ specimens.
- The performance improvement of specimens with a larger crack depth (40 mm) is found to be superior to that with a lesser crack depth (25 mm), irrespective of the geosynthetic-interlayer type. Owing to the fact that the reinforcing and membrane effects of geosynthetic interlayers are completely mobilized in specimens with larger crack depths, due to the high deformations witnessed at very few load repetitions.
- The DIC analysis suggested that the tensile strains at the crack tip were very high in CS compared to the specimens with geosynthetic-interlayers, irrespective of notch depth in the bottom layer. An average reduction in tensile strain of about 35–70% was noticed in specimens with geosynthetic interlayers.
- The maximum vertical strains are mobilized at the interface zone in the geosynthetic-reinforced asphalt specimens, as a result of horizontal crack growth in that zone. This condition leads to a possible delamination between the pavement layers.

## References

- ASTM D4595 (2009) Standard test method for determining tensile properties of geotextiles by the wide-width strip method. Annual book of ASTM standards. ASTM International, West Conshohocken, PA
- ASTM D7460 (2010) Standard test method for determining fatigue failure of compacted asphalt concrete subjected to repeated flexural bending. Annual book of ASTM standards. ASTM International, West Conshohocken, PA
- Brown SF, Thom NH, Sanders PJ (2001) A study of grid reinforced asphalt to combat reflection cracking. *J Ass Asph Paving Technol* 70:543–569
- Caltabiano MA (1990) Reflection cracking in asphalt overlays. Thesis submitted to University of Nottingham for the Degree of Master of Philosophy
- Cleveland GS, Button JW, Lytton RL (2002) Geosynthetic in flexible and rigid pavement overlay. Report 1777-1. Texas Transport Institute, Texas A&M University System
- Elsefi MA (2003) Performance quantification of interlayer systems in flexible pavements using finite element analysis. Instrument response and non destructive testing. Ph.D. thesis submitted to Virginia Polytechnic Institute and State University
- Elsefi MA, Al-Qadi IL (2003) A simplified overlay design model against reflective cracking utilizing service life prediction. *Transp. Res. Rec. J. Transp. Res. Board* No 3285

- Ferrotti G, Canestrari F, Pasquini E, Virgili A (2012) Experimental evaluation of the influence of surface coating on fiberglass geogrid performance in asphalt pavements. *Geotext Geomemb* 34:11–18
- Kumar VV, Saride S (2017) Use of digital image correlation for the evaluation of flexural fatigue behavior of asphalt beams with geosynthetic interlayers. *Transport Res Rec: J Transport Res Board* 2631:55–64
- Kumar VV, Saride S (2018) Evaluation of cracking resistance potential of geosynthetic reinforced asphalt overlays using direct tensile strength tests. *Constr Build Mater* 162:37–47
- Kumar VV, Saride S, Peddinti PRT (2017) Interfacial shear properties of geosynthetic interlayered asphalt overlays. In: *Proceedings of geotechnical frontiers-2017, Orlando, USA*
- Moreno-Navarro F, Rubio-Gamez MC (2014) UGR-FACT test for the study of fatigue cracking in bituminous mixes. *Constr Build Mater* 53:182–189
- Prieto JN, Gallego J, Perez I (2007) Application of the wheel reflective cracking test for assessing geosynthetics in anti-reflection pavement cracking systems. *Geosynth Int* 14(5):287–297
- Saride S, Kumar VV (2017) Influence of geosynthetic-interlayers on the performance of asphalt overlays placed on pre-cracked pavements. *Geotext Geomembr* 45:184–196
- Virgili A, Canestrari F, Grilli A, Santagata FA (2009) Repeated load test on bituminous systems reinforced by geosynthetics. *Geotext Geomemb* 27:187–195